Rheol Acta (2011) 50:389–402
DOI 10.1007/s00397-010-0518-x

ORIGINAL CONTRIBUTION

The influence of temperature on rheological properties of blood mixtures with different volume expanders—implications in numerical arterial hemodynamics simulations

Andreja Zupančič Valant · Lovro Žiberna · Yannis Papaharilaou · Andreas Anayiotos · Georgios C. Georgiou

Received: 11 May 2010 / Revised: 3 December 2010 / Accepted: 6 December 2010 / Published online: 22 January 2011

Abstract During the complicated cardiac surgery on a non-beating heart with cardiopulmonary bypass, protection of the heart is accomplished by injecting cold cardioplegic solutions. In most forms of circulatory shock, it is necessary to immediately restore the circulating volume. Intravenous solutions of volume expanders, such as hydroxyethyl starch and dextrans, are used to increase the volume of fluid in the circulating blood. In this work, blood samples of six donors were obtained and used to prepare mixtures with different volume expanders in concentrations ranging from 10 to 50 vol./vol.%. The flow curves of all mixtures in the temperature range from 4°C to 37°C were constructed and fitted to the Herschel–Bulkley model, in order to extract the shear thinning and yield stress parameters. To assess the influence of the observed changes in the rheological properties of blood on the hemodynamics in arterial vasculature, a realistic three-dimensional rigid-wall computational model was constructed from MRI images of the right carotid bifurcation obtained in vivo from a healthy male volunteer. The time-varying flow field was numerically computed using the Newtonian model as well as the Herschel–Bulkley model with the Papanastasiou regularization. The numerical simulations indicate only moderate changes in the time-averaged flow field that become accentuated when the instantaneous flow field is considered. We also found that although the influence of temperature, hematocrit, and volume expanders on hemodynamics is significant, this can primarily be attributed to the changes in the nominal viscosity of the flow medium.

Keywords Hemorheology · Blood · Volume expanders · Herschel–Bulkley model · Hemodynamics

Paper presented at Workshop on Viscoplastic Fluids: from Theory to Applications. November 1–5, Limassol, Cyprus.

A. Zupančič Valant (✉)
Department of Chemical, Biochemical and Environmental Engineering, University of Ljubljana, Askerceva 5, Sl-1000 Ljubljana, Slovenia
e-mail: andreja.valant@fkkt.uni-lj.si

L. Žiberna
Institute of Pharmacology and Experimental Toxicology, Faculty of Medicine, University of Ljubljana, Korytkova 2, Sl-1000 Ljubljana, Slovenia

Y. Papaharilaou
Foundation for Research and Technology Hellas (FORTH), Institute of Applied and Computational Mathematics, PO Box 1527, 71110, Heraklion, Crete, Greece

A. Anayiotos
Department of Mechanical Engineering and Materials Science and Engineering, Cyprus University of Technology, Limassol 3503, Cyprus

G. C. Georgiou
Department of Mathematics and Statistics, University of Cyprus, PO Box 20537, 1678 Nicosia, Cyprus

Introduction

Augmenting cardiac output and organ perfusion by adequate restoration of intravascular volume is of crucial importance in managing the surgical and the critically ill intensive care patients. The primary defect in all forms of circulatory shock is a critical reduction in blood flow and shear forces, which are associated with

severe rheological abnormalities. Changes in hemorheology play an important pathogenetic role and contribute to the further deterioration of the physiological state. Whole blood viscosity is mainly determined by hematocrit, whereas plasma viscosity mainly depends on the concentration of high molecular weight proteins (Koppensteiner 1996). Decreased hematocrit and loss of plasma proteins in hemorrhagic shock cause a reduction in the whole blood and plasma viscosities. Therefore, the primary goal of volume replacement therapy is to ensure stable hemodynamic conditions by rapid restoration of circulating plasma volume. This can be accomplished effectively by maintaining colloid oncotic pressure with intravenous infusions of colloid solutions.

Among common non-protein colloid solutions used as plasma substitutes are dextran and hydroxyethyl starch solutions. Most colloid solutions are presented with colloid molecules dissolved in isotonic saline, whereby colloid molecular size can be highly variable. Dextran is a mixture of glucose polymers of various sizes and molecular weights, which are neutral and water-soluble. The colloid oncotic power of dextran solutions is very high, due to a high water-binding capacity. Hydroxyethyl starches (HES) are derived from chemically modified amylopectin. They are therefore branched polysaccharides closely resembling glycogen, which are substituted with hydroxyethyl groups at carbons 2,3, and 6 of the glucose subunits. It is important to note that the extent and duration of plasma volume expansion (PVE), as well as their effects on blood rheology, the coagulation system, and other likely clinical variables, depend on the preparation of the HES, as the achieved physicochemical properties may be quite different. In addition, HES have high water-binding capacity in the same range as dextran solutions (Grocott et al. 2005).

The predominant effect of colloid solutions on blood rheology is to reduce whole blood viscosity by hemodilution, thus reducing the frictional energy losses due to the flow of blood in the vasculature and easing cardiac load. The magnitude of this effect is proportional to the degree of PVE and is larger initially for the lower molecular weights dextrans and HES. Both types of semisynthetic colloid solutions influence also plasma viscosity and red blood cell aggregation, and this contributes to their overall effects on blood rheology. The higher molecular weight dextrans and HES (such as dextran 70 and HES 200/0.5) cause an increase in plasma viscosity. This effect is smaller in magnitude than the dilutional decrease in whole blood viscosity. The lower molecular weight dextrans and HES (such as dextran 40 and HES 130/0.6) tend to cause reduced red blood cell (RBC) aggregation and plasma viscosity, thus further enhancing dilutional hypoviscosity which results in increased flow, particularly in the venous system (Neff et al. 2005).

Blood viscosity mediates the relationship between blood pressure gradients and blood flow. The velocity of blood and the range of shear rates are related to the cross-sectional area of the blood vessel. Large arteries are typically associated with higher blood flow velocities and shear rates as compared to those found in the microcirculation. Thus, under normal physiologic conditions, the viscosity of blood in the circulation, at any instant or location, varies depending on shear rate within a specific vessel. The rheological properties of blood depend on hematocrit and plasma constituents (Baskurt and Meiselman 2003). With increasing cellular fraction in blood, viscosity increases. Plasma expanders are typically Newtonian fluids of viscosity different from that of blood. They alter the rheological properties of blood as a consequence of hemodilution and its inherent physical properties. In emergency medicine, the volume expander solutions are used at room temperature.

Another clinical setting for the usage of colloid substitutes is during heart–lung perfusion in open-heart surgery, where dextrans and HES solutions may replace donor plasma as colloids. Furthermore, using dextrans and HES instead of donor plasma may be advantageous, since it allows adjustment of the colloid osmotic pressure over a wider range than donor plasma (Reed et al. 1985). In cardiac surgery, during resuscitation protocols, cold cardioplegic solutions dominate. When performing deliberate deep hypothermia for cardiac or thoracic aortic surgery requiring temporary circulatory arrest, blood temperature is in the range of 8–12°C (Eckmann et al. 2000). Since the physical characteristics of blood are complex, the rheological properties of blood at temperatures commonly used for deep hypothermia cannot be reliably predicted based on measurements at higher temperatures. Blood viscosity fluctuates dramatically in response to changes in composition, temperature and velocity, which may alter significantly within the vascular tree (Rand et al. 1964). It is important to consider the effect of temperature on the rheological behavior of blood. The pathophysiologic effects of hypothermia that induce blood hyperviscosity are still not well understood.

The objective of this work is to investigate the effects of mixing different volume expanders with whole human blood on rheological properties and, consequently, on arterial flow. The rheological properties of blood mixtures depend on the characteristics of the volume expander. When the same volume expander is mixed with blood from different donors, slight differences can be expected in flow curves at low shear rates,

due to aggregation tendencies. These depend on the plasma composition, and are mainly associated with the fibrinogen concentration. Here, we examine the influence of temperature on the rheological properties of whole blood mixtures with different volume expanders, such as solutions of dextran and HES. To that end, we have employed the Herschel–Bulkley constitutive equation, which describes well the shear thinning and yield stress characteristics of whole blood (Kim et al. 2009; Sankar and Lee 2009). In order to investigate the effects of temperature and volume expanders on the hemodynamics, we have carried out numerical simulations of the flow of various blood mixtures in a realistic carotid bifurcation using the regularized version of the Herschel–Bulkley model as well as a rescaled Newtonian model. For the cases considered in this study, the numerical simulations demonstrate that viscoplasticity affects only slightly the time-averaged flow field in the carotid artery.

Experimental methods and materials

The rheological properties of whole blood and its mixtures with volume expanders were measured under steady shear conditions in the temperature range from 4°C to 37°C, using a controlled stress rheometer Physica MCR 301, equipped with a sensor designed for hemorheology (DG 26.7/Ti). To eliminate sedimentation of RBC and the effect of the shear history of the sample and thus obtain repeatable data, the flow curves were constructed according to the following four-step protocol: pre-shear at 200 s^{-1} for 200 s, pre-shear at 1 s^{-1} for 20 s, rest conditions for 20 s, and, finally, stepwise shear rate increase from 0.5 s^{-1} to 450 s^{-1}. Blood samples were obtained by venipuncture from three (healthy) female, F1–F3, and three male, M1–M3, donors and were anticoagulated with EDTA. The hematocrit values (Hct) for all donors were determined by means of a Coulter device. As reported in Table 1, Hct values ranged from 0.36 to 0.49. It should be noted that the rheological properties of whole blood, such as shear thinning and the yield stress, are strong functions of the hematocrit (Picart et al. 1998; Yeow et al. 2002).

Table 1 The hematocrit values determined for examined blood samples

Donor code	Hematocrit
F1	0.36
F2	0.39
F3	0.39
M1	0,46
M2	0.48
M3	0.49

F female, *M* male

Table 2 Characteristics of HES volume expanders V 6, HES 6 and HES 10

Hydroxyethyl starches pH 5.5 in a 0.9% saline solution	V 6 130/0.4	HES 6 200/0.5	HES 10 200/0.5
Concentration (%)	6	6	10
Volume efficacy (%)	100	100	130
Volume efficacy duration (h)	2–3	3–4	3–4
Average molar mass (kDa)	130	200	200
Degree of substitution* (MS)	0.4	0.5	0.5
Substitution pattern C2/C6 ratio**	9:1	6:1	6:1

One hour after the venipuncture, blood samples were mixed with volume expanders at four concentrations ranging from 10 to 50 vol./vol.%. We used five different volume expanders: S40, S70, Voluven (V6), HES6, and HES10. The first two expanders were based on Soludeks®, a trade name of dextran solutions for intravenous injection, produced by Pliva, Zagreb, Croatia. S40 is 10 wt.% dextran of average molecular weight 40,000 Da dissolved in physiological fluid. S70 is 6 wt.% dextran of average molecular weight 70,000 Da dissolved in physiological fluid. The other three volume expanders used were hydroxyethyl starches, i.e., Freeflex® in saline solutions, produced by Fresenius Kabi Deutschland GmbH, Bad Homburg, Germany. The characteristics of the three HES expanders (Voluven, HES6, and HES10) are depicted in Table 2.

HES preparations differ in the number of hydroxyethyl's per number of glucose, e.g., a degree of 0.5 is equivalent to 5 hydroxyethyl starches per 10 glucose molecules. The substitution pattern C2/C6 ratio refers to the relative ratio of the hydroxyethyl starch substitutions at the carbon level and is associated with blood coagulation. Some studies have shown that at higher values of the C2/C6 ratio the negative effects on the coagulation are enhanced (Riback 2004). According to Neff et al. (2005), starches of lower molar mass (130 kDa) have less effect on coagulation than starches of medium molar mass (200 kDa).

Experimental results

The viscosities of all blood samples and volume expanders at the two extreme temperatures of interest, i.e., 4°C and 37°C, are plotted in Fig. 1 as functions of the shear rate. It is clear that blood is shear thinning in all cases, which is, of course, very well documented in

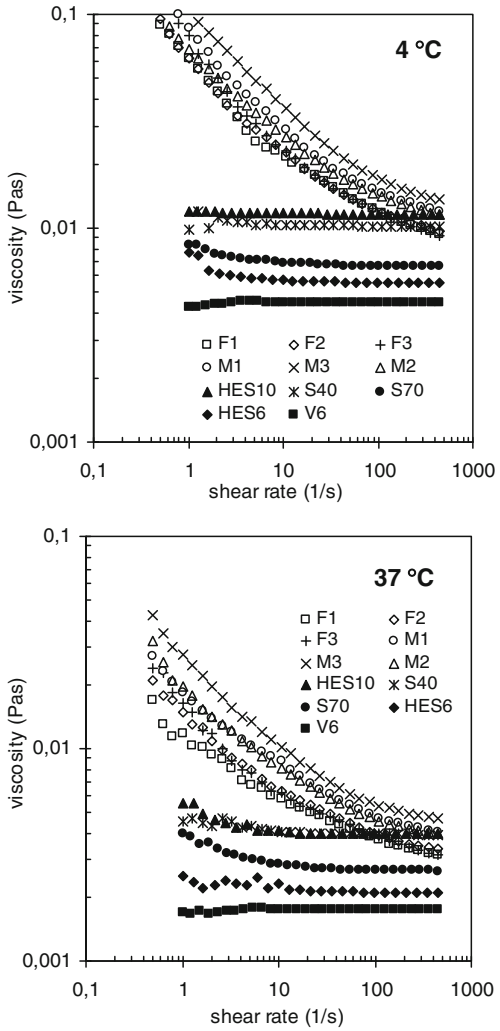

Fig. 1 The viscosities of all whole human blood samples (donors F1–F3 and M1–M3) and all volume expanders (S40, S70, HES6, HES10, and Voluven) at 4°C and 37°C

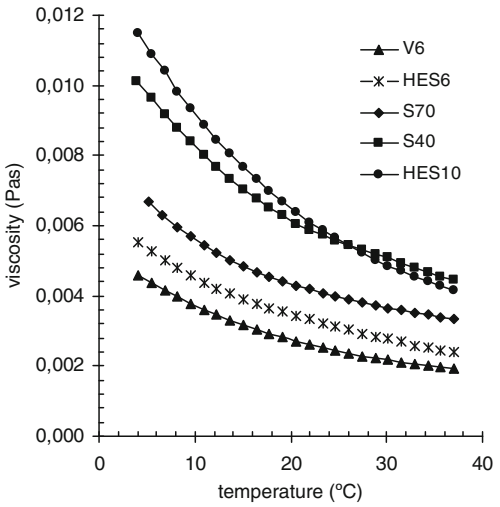

Fig. 2 Temperature dependence of the viscosities of all volume expanders at a shear rate of 100 s^{-1}

the literature (Neofytou and Drikakis 2003; Neofytou 2004; Sankar and Lee 2008 and references therein), whereas volume expanders are essentially Newtonian at moderate to high shear rates. At low shear rates, some volume expander solutions, such as Voluven, HES6, and S70, exhibit weak shear thinning behavior which is more pronounced at the higher temperature (37°C). It should also be noted that the viscosity values of the volume expanders obtained at low shear rates (below 1 s^{-1}) are not reliable and are thus omitted. For all donors, the viscosity of whole human blood is higher than that of volume expander solutions considered in this work, at least for low and moderate shear rates. The differences are reduced as the shear rate is increased and the viscosity curves may cross at high shear rates. As expected, increasing the temperature from 4°C to 37°C results in a drastic reduction of the viscosity at all shear rates. Figure 2 shows the viscosities of all volume expanders at a constant shear rate of 100 s^{-1} as functions of the temperature. HES10 and S40, i.e., the 10% saline solutions, exhibit higher viscosity than the 6% solutions, i.e., S70, HES6, and Voluven.

The effect of the concentration of medium molecular weight volume expanders on the viscosity of blood mixtures at 4°C and 37°C is illustrated in Figs. 3 and 4. In Fig. 3, we present viscosity results for whole blood M1, which is characterized but its high hematocrit (Hct = 0.46), and its mixtures with volume expander HES10 at concentrations ranging from 10% to 50%. In Fig. 4, we have chosen to show results obtained with whole blood F1, which exhibits low hematocrit (Hct = 0.36), and its mixtures with S70. The viscosity curves obtained with other blood samples and volume expanders were similar. In general, the viscosity at low shear rates decreases with the addition of a volume expander, due to hemodilution. The shear thinning behaviour is reduced with increasing concentration of volume expanders. It is evident in Fig. 3 that the differences between the viscosity curves in the low-shear-rate regime are more pronounced at low temperatures. Our experiments indicated that adding the same volume expander to different blood samples causes slightly different changes in the viscosity, due to different fibrinogen concentration and other constituents present in plasma. More important differences were observed mainly at low shear rates, where aggregation tendencies or viscosity increase were also noted. In Fig. 4, for example, we notice that the low-shear-rate viscosity of whole blood F1 at 37°C is slightly

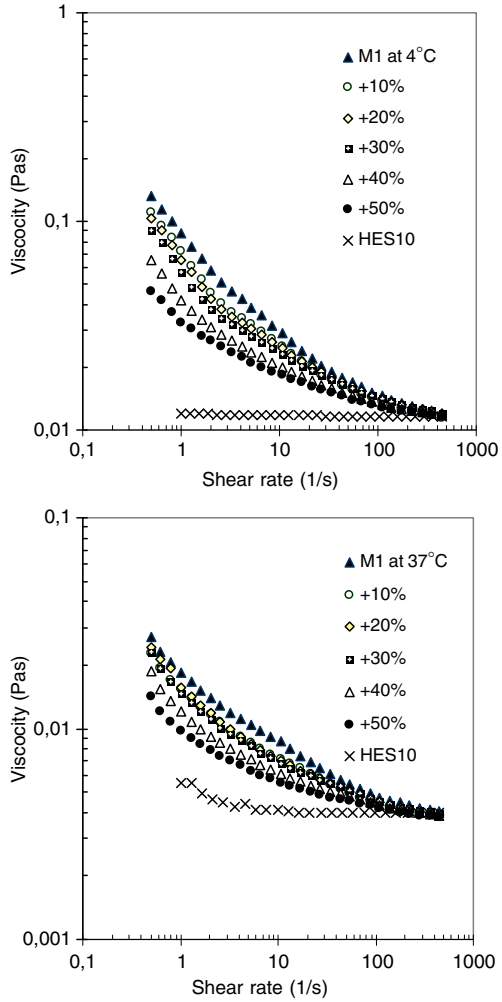

Fig. 3 The viscosities of whole human blood sample M1 (Hct = 0.46) and its mixtures with 10 to 50 vol.% of HES10 at 4°C and 37°C; the viscosity of HES10 is also shown

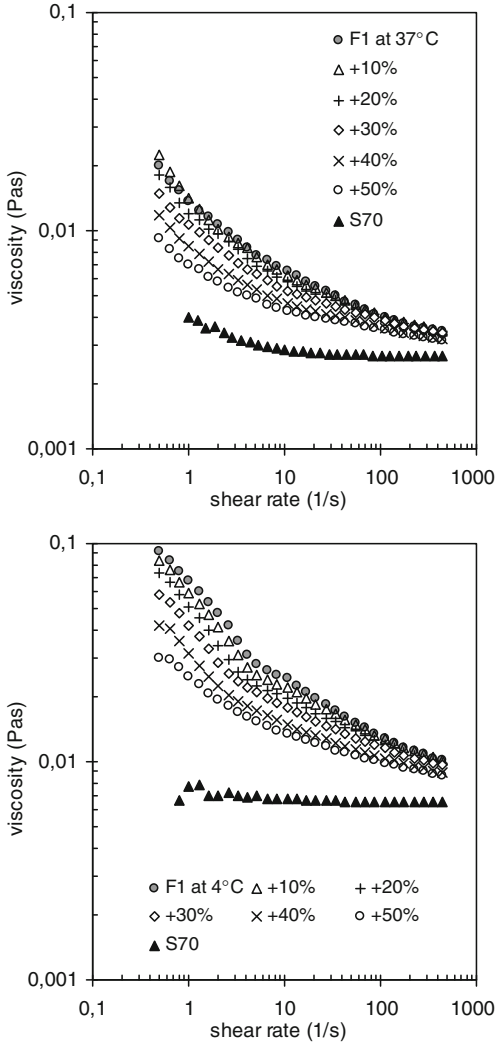

Fig. 4 The viscosities of whole human blood sample F1 (Hct = 0.36) and its mixtures with 10 to 50 vol.% of S70 at 4°C and 37°C; the viscosity of S70 is also shown

below that of its mixture with 10% S70. Another general observation is that RBC aggregation tendencies in blood mixtures with volume expanders are not common, indicating that hemodilution prevails over the aggregation.

In order to examine in more detail the effect of volume expanders on the viscosity of the different whole blood samples, we calculated the values of the *relative viscosity*, defined as the ratio of the viscosity of the blood mixture to that of the blood at a given shear rate. In Fig. 5, we show the average relative viscosities of various mixtures of blood samples F3, M1, and M2 at 4°C and 10% of volume expander (Fig. 5a), 4°C and 40% of volume expander (Fig. 5b), and 37°C and 40% of volume expander (Fig. 5c). The results at low shear rates and low volume expander concentrations show no clear trend of the relative viscosity as a function of the shear rate. In general, the relative viscosity is an increasing function of the shear rate, exceeding unity at very high shear rates. With the exception of some mixtures at very high shear rates (above 100 s^{-1}), the relative viscosity is reduced as the volume expander concentration is increased. This reduction is more striking at low shear rates. At higher shear rates, some blood mixtures with S40 and HES10 exhibit viscosities higher than that of the whole human blood (the average relative viscosities are higher than 1). Finally, the reduction of the viscosity due to plasma dilution with examined volume expanders was more pronounced at 4°C, except for Voluven, which had the lowest viscosity. As discussed below, however, this reduction is accompanied with an increase of the yield stress.

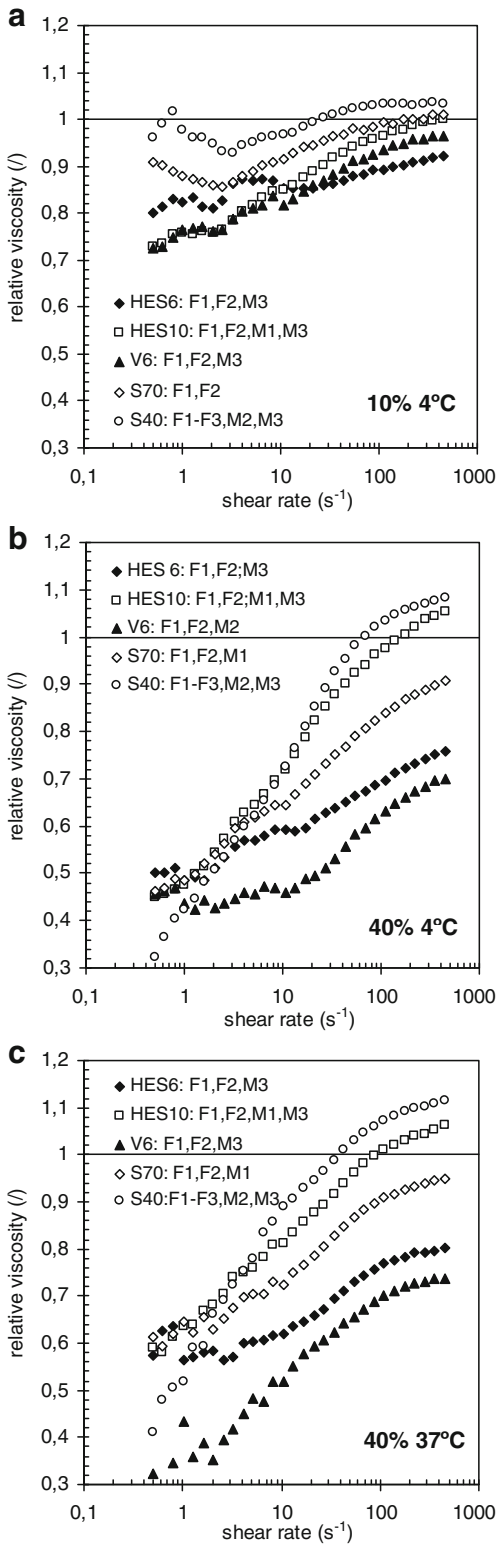

Fig. 5 Average relative viscosities of some blood mixtures with different volume expanders: **a** 10% of volume expander at 4°C, **b** 40% of volume expander at 4°C, and **c** 40% of volume expander at 37°C

Constitutive equation

In addition to shear thinning, blood is known to exhibit yield stress (Kim 2002; Sankar and Lee 2008). This was also true for all blood samples and mixtures in the present work. The viscosity curves of the whole blood samples in Fig. 1 as well as those of the various blood mixtures with volume expanders in Figs. 3, 4, and 6, appear to increase without limit for small shear rates. As pointed out by Yeow et al. (2002), this asymptotic behavior is indicative of the presence of yield stress. We chose to fit the rheological data with the well-known Herschel–Bulkley model. This is a combination of the Bingham and power-

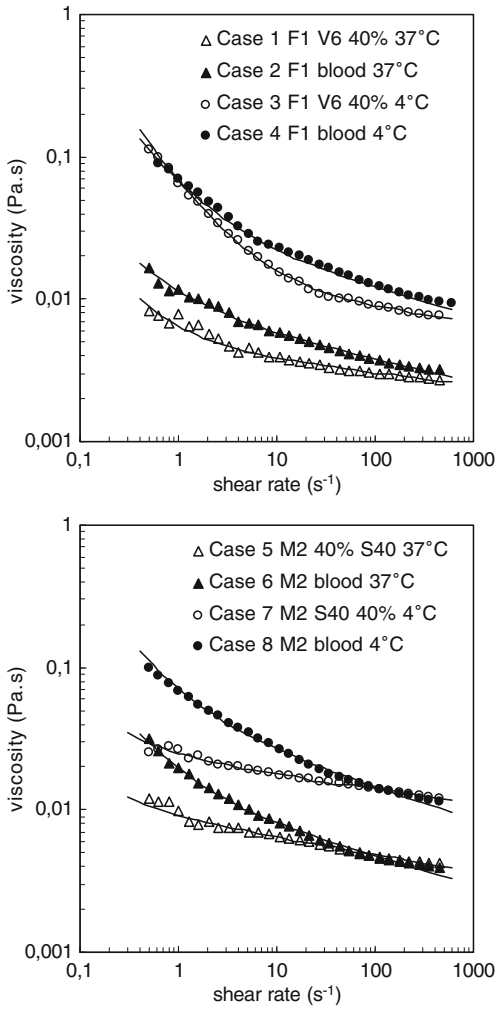

Fig. 6 The viscosity curves of blood samples and mixtures (cases 1–8) used in numerical modeling. The points are the experimental data and the lines are calculated using the Hershel–Bulkley model. The material parameters are given in Table 3

law models and can be written in the following scalar form:

$$\begin{cases} \dot{\gamma} = 0, & \tau < \tau_0 \\ \tau = \tau_0 + K\dot{\gamma}^n, & \tau \geq \tau_0 \end{cases} \quad (1)$$

where τ is the shear stress, $\dot{\gamma}$ is the shear rate, K is the consistency index, n is the power-law exponent, and τ_0 is the yield stress. The values of the three material parameters of the Herschel–Bulkley model, i.e., K, n, and τ_0,have been determined from the rheological data of each fluid using non-linear regression (Excel Solver). In Table 3, we tabulate the values of the material parameters for eight cases, obtained with two blood samples (F1 and M2) at 4°C and 37°C and their mixtures with 40% Voluven (V6) and S40, respectively. The two blood samples were chosen because they exhibit extreme hematocrit values (Hct = 0.36 for F1 and Hct = 0.48 for M2). Among the volume expanders examined, Voluven and S40 had the lowest and highest viscosity, respectively. Although these two volume expanders have been reported to reduce RBC aggregation (Neff et al. 2005; Salazar Vázquez et al. 2008), in the present work we observed a tendency for aggregation in blood sample F1 with Voluven at 4°C. This can be recognized from the relatively high yield stress and viscosity measured in the low shear rate range. S40 in the blood mixtures examined exhibited only a dilutional effect.

The experimental data for the cases 1–8 of Table 3 and the flow curves calculated using the Herschel–Bulkley model are compared in Fig. 6. In Table 3, we observe that the calculated power-law exponents were in the range 0.78–0.92. The yield stress values, ranged from 0.0008 to 0.0562 Pa, are reduced with temperature or with the addition of a volume expander, the only exception being the mixture of blood F1 with Voluven at 4°C which exhibits higher yield stress than the whole blood. It should be noted that in order to obtain more reliable values for the yield stress the rheological measurements should be extended to much lower shear rates than 0.1 s^{-1} (Yeow et al. 2002). Such a task falls out of the scope of this preliminary study of the effects of volume expanders. However, the calculated material parameters for the blood samples compare well with values reported in the literature. For example, Kim (2002) reported the values $\tau_0 = 0.0175$ Pa, $n = 0.8601$, and $K = 8.9721$ Pa s^n. According to Sankar and Hemalathan (2007) the yield stress for a normal human blood is between 0.01 and 0.06 Pa and the typical values of the power-law exponent n are between 0.9 and 1.1.

Table 3 Herschel–Bulkley model parameters obtained from stress strain measurements of human blood samples at 4°C and 37°C and including or excluding volume expanders

HB model parameters	Blood F1 + 40% Voluven at 37°C	Blood F1 at 37°C	Blood F1 + 40% Voluven at 4°C	Blood F1 at 4°C	Blood M2 + 40% S40 at 37°C	Blood M2 at 37°C	Blood M2 + 40% S40 at 4°C	Blood M2 at 4°C
Case #	1	2	3	4	5	6	7	8
τ_0 [Pa]	0.0021	0.0035	0.0562	0.0340	0.0008	0.0082	0.0029	0.0330
K [Pa s^n]	0.0044	0.0080	0.0125	0.0283	0.0084	0.0115	0.0221	0.0386
n []	0.9167	0.8375	0.9144	0.8097	0.8790	0.8033	0.8995	0.7827

The blood sample F1 used for cases 1–4 had Hct = 0.36 whereas the sample M2 used for cases 5–8 had Hct = 0.48

Numerical modeling of arterial hemodynamics

The carotid bifurcation has been selected for our numerical hemodynamics simulations, as it is one of the most frequently studied sites evaluating the hemodynamic hypothesis of atherosclerosis. Computations have been carried out for the eight cases of whole human blood and blood mixtures provided in Table 3.

Using a 3.0-T Philips Achieva MRI instrument, a series of thin sequential slices were obtained by 3D time of flight (TOF) methods, covering the carotid artery bifurcation of a healthy volunteer in the supine position. The inflow and outflow boundary conditions were obtained by MR phase contrast velocimetry (Papaharilaou et al. 2001) at the limits of the TOF covered anatomic region. Segmentation and 3-D surface reconstruction of the MR images were performed using purpose-developed software (Giordana et al. 2005). The surface of the 3-D true vessel lumen was reconstructed from the segmented TOF images. Pixel width constrained smoothing of the reconstructed surfaces was applied and smoothly matched cylindrical extensions of both inflow and outflow segments were added to facilitate the application of fully developed boundary conditions for the numerical simulation. Further details on the image acquisition and 3D surface reconstruction methods can be found in Aristokleous et al. (2011).

In order to solve numerically the continuity and momentum equations governing the three-dimensional, time-dependent incompressible flow, we used the finite volume code Fluent v12.0 (Ansys Inc.). The computational grids were generated with ANSA v12 (Beta CAE Systems, Greece) using $\sim 7.5 \times 10^5$ mixed type elements with higher grid density in the vicinity of the bifurcation and a $0.055R$ thick viscous layer adjacent to the wall, where $R = 2.927 \times 10^{-3}$ m is the inlet carotid radius. The arterial wall was assumed rigid and blood and its mixtures were modeled as incompressible fluids with a density $\rho = 1050$ kg/m^3.

A 0.65/0.35 internal carotid artery (ICA)/ECA flow split was prescribed based on the in vivo MR phase contrast velocimetry measurements. From the discrete Fourier series of the volumetric flow rate measured in vivo by MRI (Fig. 7), the fully developed, time-varying velocity profile was computed using Womersley's derivation (Womersley 1955) and was then imposed as the time-dependent inflow boundary condition. The spatiotemporally-averaged Reynolds number is defined as $Re_m = 2\rho\bar{u}R/\eta_\infty$, where $\bar{u}$ is the time-averaged mean inlet velocity and η_∞ is the limiting high-shear-rate Newtonian viscosity, which is

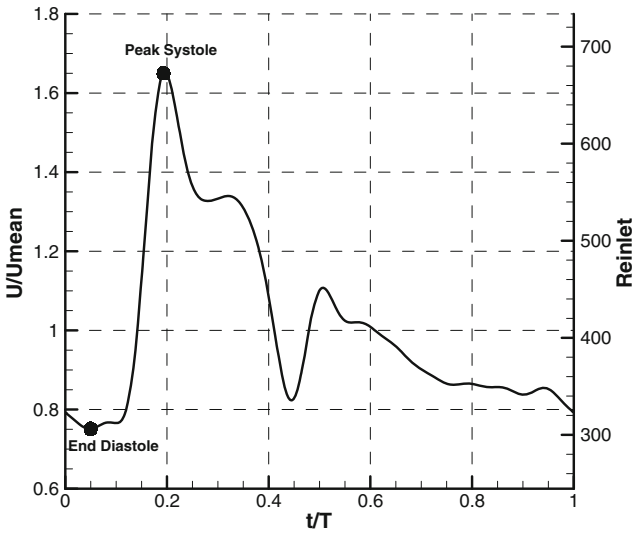

Fig. 7 Physiologic flow waveform applied for time-varying computations. Reynolds number computed for Newtonian model ($\eta_\infty = 3.5$ cP). Mean inlet velocity U normalized with spatiotemporal mean inlet velocity $U_{\text{mean}} = 0.23$ m/s

taken here as 3.5 cP. This value is the most common value used in the literature for blood flow simulations (Kim 2002; Shibeshi and Collins 2005). For the in vivo MR measured flow waveform shown in Fig. 7, the period is $T = 1.032$ s and the measured time-averaged volumetric flow rate is $Q = 6.247$ ml/s, which yields $\bar{u} = 0.232$ ms^{-1}. The time-averaged Reynolds number at the inlet turns out to be $Re_{\text{m}} = 403.9$. The Womersley parameter, defined by $\alpha = R(\omega/\nu)^{1/2}$, where $\omega = 2\pi$/T is the fundamental frequency and ν is the (high-shear-rate) kinematic viscosity, was $\alpha = 3.96$. A second-order upwind discretization scheme (Barth and Jespersen 1989) was applied for both the momentum and pressure equations, and the PISO scheme (Issa 1986) was used for pressure velocity coupling. A time periodic solution was achieved after three flow cycles.

A systematic time step and grid size independence study was carried out following the approach described in Papaharilaou et al. (2007). Based on the test results carried out in this study, a time step of $\Delta t = 6.5 \times 10^{-6}$ (normalized by the spatiotemporal mean inlet velocity per inlet diameter), or 4,000 time steps per flow cycle, and a spatial discretization of the computational domain with $\sim 7.5 \times 10^5$ elements proved to ensure sufficient accuracy of the numerical simulations.

Since the Herschel–Bulkley model defined in Eq. 1 is discontinuous, it requires the determination of the yielded ($\tau \geq \tau_0$) and unyielded ($\tau < \tau_0$) regions

Table 4 The characteristic viscosities for the cases from 1 to 8 calculated for the following data: Q = 6.247 ml/s, $\overline{u} = 0,23\ s^{-1}$ and $\dot{\gamma}_c = 201.8\ s^{-1}$

Case #	1A	2A	3A	4A	5A	6A	7A	8A
Characteristic viscosity (N s m^{-2})	0.002854	0.003375	0.008235	0.010476	0.004424	0.004089	0.012979	0.012346

of the flow, which leads to considerable computational difficulties. These are overcome by employing its regularized version, as proposed by Papanastasiou (1987):

$$\tau = \tau_0 \left(1 - e^{-m\dot{\gamma}}\right) + K\dot{\gamma}^n \tag{2}$$

where m is the regularization parameter. For sufficiently large values of m, the regularized constitutive model provides a satisfactory approximation of the Herschel–Bulkley model, while at the same time the need of determining the yielded and the unyielded regions is eliminated. Regularized models have been very successful in solving various steady and time-dependent flows [see, for example, Mitsoulis (2007) and the references therein]. In the present calculations we have taken $m = 1{,}000$ s.

For comparison purposes, we have also carried out simulations assuming that the fluids of interest are Newtonian with a viscosity rescaled to a value corresponding to the characteristic shear rate (not the nominal high shear rate value). In the latter case, the viscosity is rescaled as follows:

$$\eta_c = \eta\left(\dot{\gamma}_c\right) = \frac{\tau_0}{\dot{\gamma}_c}\left(1 - e^{-m\dot{\gamma}_c}\right) + K\dot{\gamma}_c^{n-1} \tag{3}$$

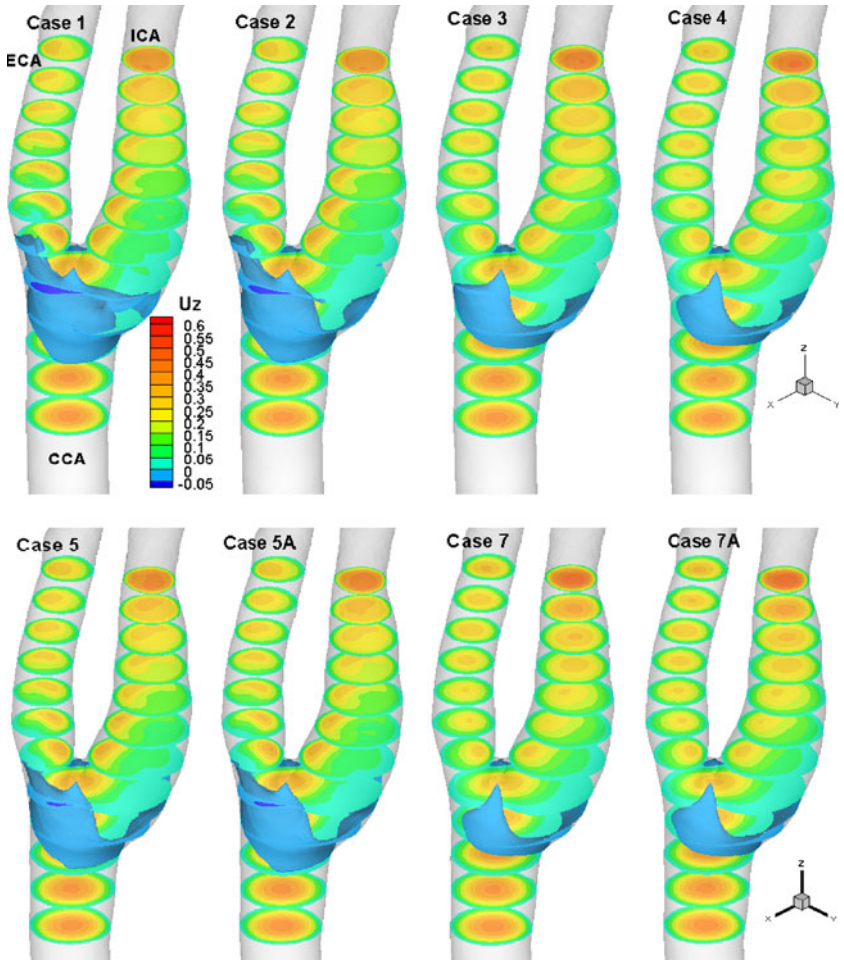

Fig. 8 Steady axial velocity contour plots obtained using the regularized Herschel–Bulkley model for cases 1–4 (Hct = 0.36) and 5 and 7 (Hct = 0.48) and the rescaled Newtonian model for the latter two cases (5A and 7A). The velocity values are in m/s and the zero isosurfaces highlight regions of flow reversal

where the characteristic shear rate is defined by $\dot{\gamma}_c = 8\bar{u}/(3R) = 201.8\ \mathrm{s}^{-1}$. The characteristic viscosities for the cases 1–8 of Table 3 are tabulated in Table 4.

The axial velocity contours obtained using the regularized Herschel–Bulkley model for cases 1–5 and 7 of Table 3 are shown in Fig. 8. Also shown is a comparison with the results obtained the rescaled Newtonian model for cases 5 and 7 (5A and 7A). Cases 6 and 8 had no visible differences from cases 5 and 7, respectively, and are therefore not shown. To highlight regions of flow reversal, the zero velocity isosurfaces are also depicted. Regions of flow reversal appear near the wall, to some extent, in all cases presented with flow separation occurring near the location of sudden cross-sectional expansion in the common carotid artery (CCA; the parent vessel in the carotid bifurcation). However, there are differences between cases in the size of the recirculation region that develops and the magnitude of the flow reversal. These differences in the flow field can primarily be attributed to the differences in the characteristic viscosity of the cases studied.

In Fig. 9, the contours of the log of wall shear stress (WSS) magnitude are shown for the same cases as those in Fig. 8. The wall shear stress is a very important hemodynamic quantity, which is defined as follows:

$$\mathrm{WSS} = \eta(\dot{\gamma}) \left.\frac{\partial u_t}{\partial n}\right|_{\mathrm{wall}} \tag{4}$$

where u_t is the tangential velocity and n is the normal unit vector at the wall. Atherosclerosis shows preferential localization at sites where flow is either slow or disturbed and where WSS as well as its gradients are low (Caro et al. 1971; Malek et al. 1999). It is evident from the steady flow WSS distributions of Fig. 9 that there is a positive correlation between the characteristic viscosity of the fluid used in each case and the resulting WSS magnitude. There is, however, a slight deviation

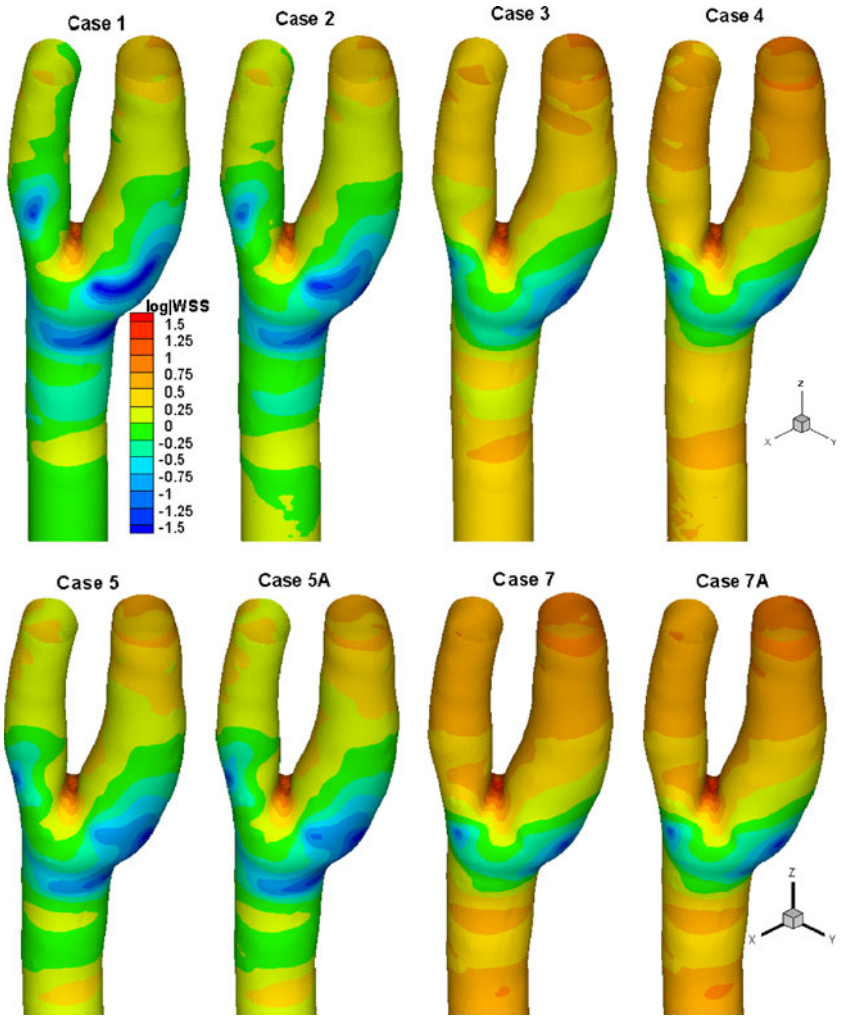

Fig. 9 Steady WSS contour plots (in Pa) obtained using the regularized Herschel–Bulkley model for cases 1–4 (Hct = 0.36) and 5 and 7 (Hct = 0.48) and the rescaled Newtonian model for the latter two cases (5A and 7A)

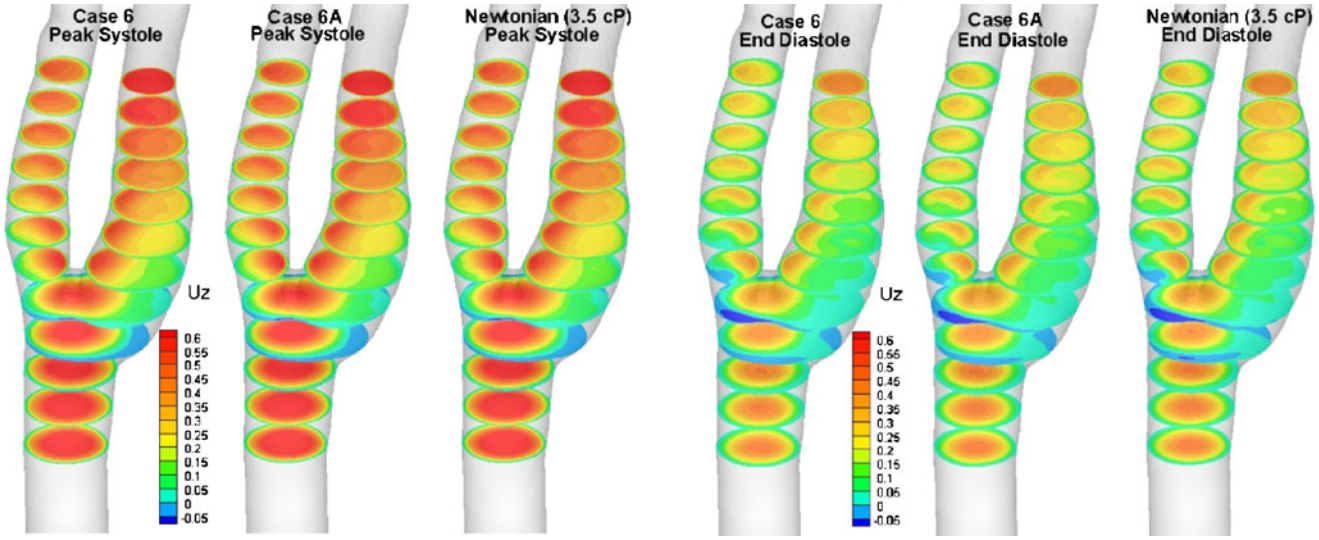

Fig. 10 Comparison of the axial velocity contours at peak systole and end diastole obtained using the regularized Herschel–Bulkley, the rescaled Newtonian, and the Newtonian models for case 6 (Hct = 0.48)

from this general observation which appears in the WSS distribution of the external carotid artery (ECA; typically the smaller diameter branch of the carotid bifurcation). There is lateral translation of an isolated low WSS region associated more with the change in Hct rather than change in characteristic viscosity (compare case 1 vs. case 5).

It is evident from the results presented in Figs. 8 and 9 that the rescaled Newtonian approximation yields a description of the flow field that is very close to that generated by the regularized Herschel–Bulkley model. This could not have been achieved by a constant viscosity approximation, especially in cases where the characteristic viscosity of the blood mixture deviates significantly from the physiological range (i.e., case 7).

Although the influence of temperature, hematocrit, and volume expanders on the hemodynamics is significant, this is primarily attributed to the net effect of these parameters on the nominal (high shear rate)

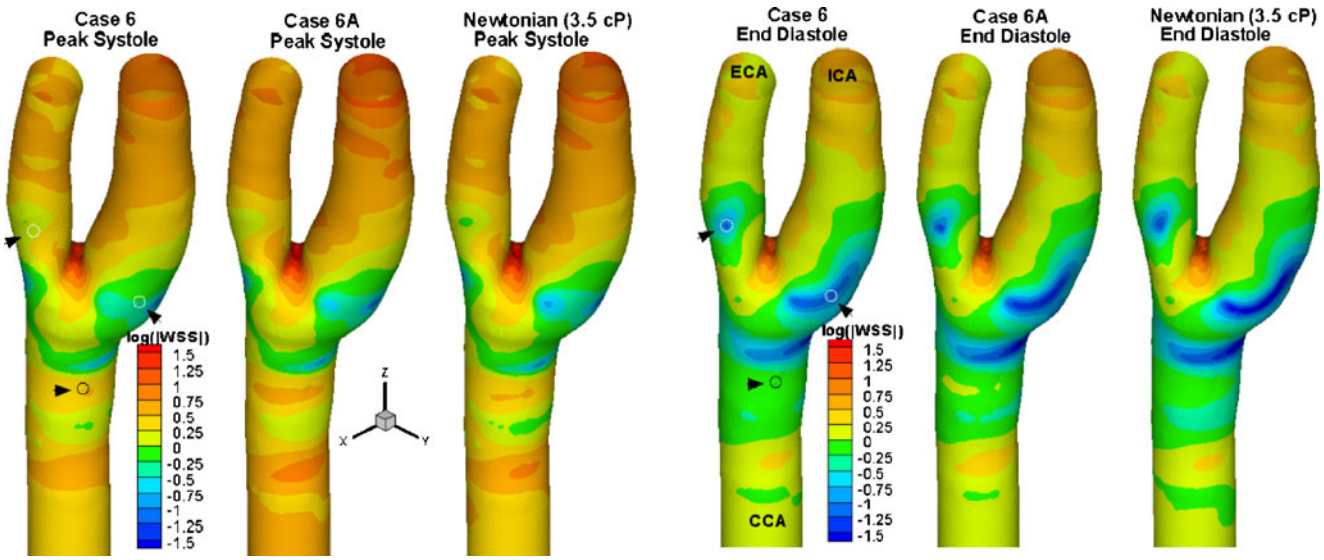

Fig. 11 Comparison of the WSS contours (in Pa) at peak systole and end diastole obtained using the regularized Herschel–Bulkley, the rescaled Newtonian, and the Newtonian models for case 6 (Hct = 0.48). The circles denote characteristic wall locations on the CCA, ECA, and ICA selected for the extraction of the time series data shown in Fig. 12

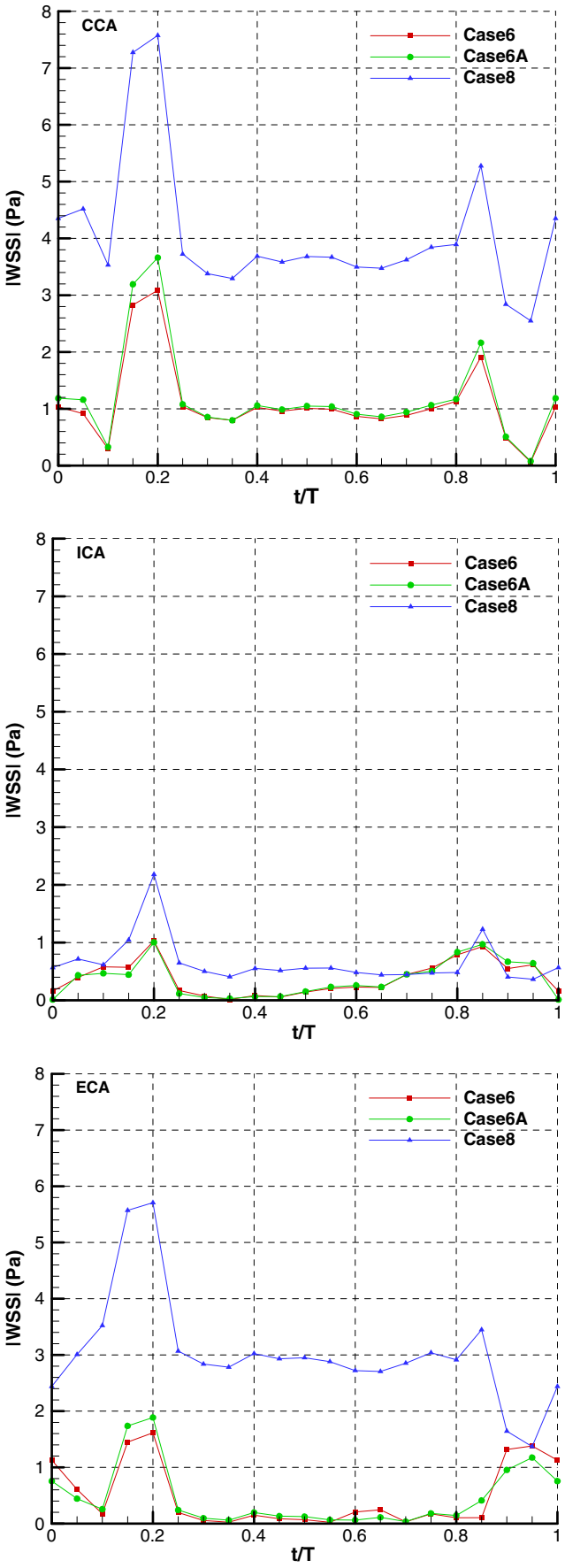

◀ **Fig. 12** Comparison of WSS time series obtained at selected points on the CCA, ICA and ECA wall (depicted in Fig. 11) using the regularized Herschel–Bulkley model for cases 6 and 8 (Hct = 0.48) and the rescaled Newtonian model (case 6A)

viscosity of the flow medium and less so on their effect on its non-Newtonian rheological behavior. If one seeks to compute the hemodynamics in a normal arterial segment, rescaling the Newtonian viscosity using the characteristic shear rate will produce a description of the hemodynamics, which is very close to that obtained by the regularized Herschel–Bulkley model. Figures 10 and 11 show a comparison of the axial velocity and the WSS contours, respectively, obtained applying the regularized Herschel–Bulkley, the rescaled Newtonian, and the Newtonian models at two characteristic instances in the cardiac cycle depicted in Fig. 7: (a) peak systole and (b) end diastole for case 6 (with Hct = 0.48). We observe that that there are no significant differences in the axial velocity and WSS results obtained with the three models. This is mainly due to the fact that the characteristic viscosity in this case ($\eta_c \sim$ 4.1 cP) is very close to the Newtonian viscosity used (3.5 cP).

Finally, Fig. 12 shows the flow cycle variation of the WSS magnitude extracted at three representative points on the CCA the ECA, and the ICA. These three points are marked by circles and indicated by arrows in Fig. 11. The results obtained using the regularized Herschel–Bulkley and the rescaled Newtonian models agree very well during most of the flow cycle. As expected, there is a consistently increased WSS level associated with the increased characteristic viscosity of case 8 as compared to cases 6 and 6A. Interestingly, this trend breaks down during the end diastolic phases on the ICA. This behavior could be attributed to the different rheological characteristics of blood between cases 6 and 8, which are expected to become more apparent during the low flow phases of the cycle.

Conclusions

Addition of examined volume expanders to whole human blood, in general, caused disaggregation of RBC, which results in the reduction of viscosity at low shear rates. Shear thinning and yield stress were reduced with the increasing concentrations of the studied volume expanders. In most blood samples examined, the aggregation tendencies of RBC due to the addition of volume expander were not significant, probably due to the prevailing effect of plasma dilution. This finding is

important for the clinical settings where it is necessary to immediately restore the circulating volume at room temperature with practically no time available to select the most appropriate type of solution. On the other hand, the viscosity differences between whole human blood and blood mixtures with different volume expanders were more pronounced at low temperature. This is important when deliberate deep hypothermia for cardiac or aortic surgery is performed, since cold cardioplegic solutions are used in a well-planned procedure that allows enough time to select the most appropriate volume expander. For that reason, potential risk by increased tendency for aggregation at low temperatures, e.g., as observed in the present experiments with Voluven, must be avoided by the proper choice of volume expander before the start of cardiac surgery or other extensive surgery. Since observed RBC aggregation tendencies in blood mixtures with volume expanders were not common, indicating that hemodilution prevails over the aggregation, it is deduced that, in general, employing cold volume expanders during cardiac surgery is safe. Nevertheless, hemorheological behavior is affected by a number of patient's individual characteristics, among which plasma proteins are a major component. Changes in fibrinogen and immunoglobulins, under both physiologic and pathologic conditions exert their effects on whole blood viscosity either directly or by influencing red cell aggregation and platelet thrombogenesis (Kwaan 2010). These factors must be studied in more detail since the most pronounced inter-individual changes in rheological parameters were observed mainly at low shear rates. In this range of shear rates, blood exhibits flow properties of structured fluid due to RBC aggregation, while their deformability plays a lesser role.

As such interactions are very complex, we employed numerical arterial hemodynamics simulations, in order to investigate further the observed temperature-dependent differences in in silico model of carotid circulation. The Herschel–Bulkley constitutive equation describes well the viscosity data of all samples within the applied shear rate region from 0.1 to 1,000 s^{-1}. Our numerical simulations of the flow of whole blood and its mixtures with volume expanders in the carotid bifurcation demonstrated the following: (a) taking into account the viscoplasticity of blood (i.e., its yield stress) results only in moderate changes in the time-averaged flow field in the carotid artery; these changes are more pronounced in the case of the instantaneous flow field; (b) rescaling the Newtonian viscosity using the characteristic shear rate leads to a satisfactory description of the flow of a Herschel–Bulkley fluid in the carotid artery; this implies that the effects of temperature, hematocrit, and volume expander concentration can be attributed to the variation of the characteristic viscosity of the fluid.

The observed differences in the rheological behavior of whole blood and blood mixtures with volume expanders can be translated, e.g., in a setting of cardiopulmonary bypass, where a variety of hematocrit concentrations and temperatures are encountered. Therefore, the present results raise an important issue about the potential clinical complications and suggest that choosing the plasma expanders according to the patients' individual plasma characteristics could improve the safety of complicated cardiac surgery. Since these issues are not yet well documented nor well understood, further investigation in this field is needed.

Acknowledgements The project was partially funded by two Cyprus–Slovenia grants from the Cyprus Research Promotion Foundation and the Slovenia Research Agency (Projects CY-SLO/0407/05 and CY-SLO/0609/01).

References

Aristokleous N, Seimenis I, Papaharilaou Y, Georgiou G, Brott BC, Anayiotos AS (2011) Effect of posture change on the geometric features of the healthy carotid bifurcation. IEEE Trans Inf Technol Biomed (in press)

Barth TJ, Jespersen D (1989) The design and application of upwind schemes on unstructured meshes. AIAA 27th Aerospace Sciences Meeting, Reno, Nevada. Technical Report AIAA-89-0366

Baskurt OK, Meiselman HJ (2003) Blood rheology and hemodynamics. Semin Thromb Hemost 29:435

Caro CG, Fitz-Gerald JM, Schroter RC (1971) Atheroma and arterial wall shear. Observation, correlation and proposal of a shear dependent mass transfer mechanism for atherogenesis. Proc Roy Soc B 177:109

Eckmann DM, Bowers S, Stecker M, Cheung AT (2000) Hematocrit, volume expander, temperature, and shear rate effects on blood viscosity. Anesth Analg 91:539

Giordana S, Sherwin SJ, Peiro J, Doorly DJ, Papaharilaou Y, Caro CG, Watkins N, Cheshire N, Jackson M, Bicknall C, Zervas V (2005) Automated classification of peripheral distal by-pass geometries reconstructed from medical data. J Biomech 38:47

Grocott MPW, Mythen MGM, Gan Tong J (2005) Perioperative fluid management and clinical outcomes in adults. Anesth Analg 100:1093

Issa RI (1986) Solution of implicitly discretized fluid flow equations by operator splitting. J Comput Phys 62:40

Kim S (2002) A study of non-Newtonian viscosity and yield stress of blood in a scanning capillary-tube rheometer. PhD Thesis, Drexel University, USA

Kim S, Namgung B, Kai Ong P, Cho YI, Chun KJ, Lim D (2009) Determination of rheological properties of whole blood with a scanning capillary-tube rheometer using constitutive models. J Mech Sci Tech 23:1718

Koppensteiner R (1996) Blood rheology in emergency medicine. Semin Thromb Hemost 22:89
Kwaan (2010) Role of plasma proteins in whole blood viscosity: a brief clinical review. Clin Hemorheol Microcirc 44(3):167
Malek AM, Alper SL, Izumo S (1999) Hemodynamic shear stress and its role in atherosclerosis. J Am Med Assoc 282:2035
Mitsoulis E (2007) Flows of viscoplastic materials: Models and computations. Rheology Reviews, The British Society of Rheology, 135
Neff TA, Fischler L, Mark M, Stockler R, Reinhart WH (2005) The influence of two different Hydroxyethyl Starch solutions (6% HES 130/0.4 and 200/0.5) on blood viscosity. Anesth Analg 100:1773
Neofytou P (2004) Comparison of blood rheological models for physiological flow simulation. Biorheology 41:693
Neofytou P, Drikakis D (2003) Effects of blood models on flows through a stenosis. Int J Numer Methods Fluids 43:597
Papaharilaou Y, Sherwin SJ, Doorly DJ (2001) Assessing the accuracy of two-dimensional phase-contrast MRI measurements of complex unsteady flows. J Magn Reson Imaging 14:714
Papaharilaou Y, Ekaterinaris J, Manousaki E, Katsamouris A (2007) A decoupled fluid structure approach of estimating wall stress in abdominal aortic aneurysms. J Biomech 40:367
Papanastasiou TC (1987) Flows of materials with yield. J Rheol 31:385
Picart C, Piau JM, Galliard H, Carpentier P (1998) Human blood shear yield stress and its hematocrit dependence. J Rheol 42:1
Rand PW, Lacombe E, Hunt HE, Austin WH (1964) Viscosity of normal human blood under normothermic and hypothermic conditions. J Appl Physiol 19:117
Reed RK, Lilleaasen P, Lindberg H, Stokke O (1985), Dextran 70 versus donor plasma as colloid in open-heart surgery under extreme haemodilution. Scand J Clin Lab Invest 45:269
Riback W (2004) Plasma expanders: hydroxyethyl starches vs. gelatine www.traumasa.co.za/files%5CPlasma%20Expanders%20Botswana.pdf
Salazar Vázquez BY, Cabrales P, Intaglietta M (2008) The beneficial effects of increasing blood viscosity. Yearb Intensive Care Emerg Med 2008:691
Sankar DS, Hemalathan K (2007) Non-linear mathematical models for blood flow through tapered tubes. Appl Math Comput 188:567
Sankar DS, Lee U (2008) Two-fluid Herschel–Bulkley model for blood flow in catheterized arteries. J Mech Sci Tech 22:1008
Sankar DS, Lee U (2009) Two-fluid non-Newtonian models for blood flow in catheterized arteries—a comparative study. J Mech Sci Tech 23:2444
Shibeshi SS, Collins WE (2005) The rheology of blood flow in a branched arterial system. Appl Rheol 15:398
Womersley JR (1955) Method for the calculation of velocity, rate of flow and viscous drag in arteries when the pressure gradient is known. J Physiol 127:553
Yeow YL, Wickramasinghe SR, Leong YK, Han B (2002) Model-independent relationships between hematocrit, blood viscosity, and yield stress derived from Couette viscometry data. Biotechnol Prog 18:1068